When mixtures of hard-sphere-like colloids do not behave as mixtures of hard spheres

Ph. Germain, J. G. Malherbe, and S. Amokrane
Groupe de Physique des Milieux Denses, Faculté des Sciences et Technologie, Unviersité Paris XII–Val de Marne, 61 Avenue du Général de Gaulle, 94010 Créteil Cedex, France
(Received 14 June 2003; published 29 October 2004)

The validity of the concept of "hard-sphere-like" particles for mixtures of colloids is questioned from a theoretical point of view. This concerns the class of pseudobinary mixtures in which the nonsteric interactions between the colloids are "residual" (with very small range and moderate strength). It is shown that contrary to common expectation, such interactions may have unexpected consequences on the theoretical phase diagram. The distinction between this situation and true solute-solvent mixtures is emphasized.

DOI: 10.1103/PhysRevE.70.041409 PACS number(s): 82.70.Dd, 64.70.−p, 61.20.Gy

I. INTRODUCTION

The concept of "hard-sphere-like" colloids refers to macroparticles that are thought of as interacting mostly through a harsh repulsion associated with the particle cores. In recent years, it has been applied to the analysis of numerous pseudobinary colloidal mixtures, that is, suspensions involving two supramolecular species in a suspending medium. The underlying criterion assumes a hard-core diameter that is much greater, for both species, than any other characteristic length of the suspension (solvent or small ion diameters, thickness of the colloids surface layer, screening length, etc). This includes a large number of sterically stabilized mixtures, charge stabilized ones with a short screening length, and some that combine both mechanisms. Typical examples are mixtures of polymethylmethacrylate (PMMA) and polystyrene (PS) spheres, or mixtures of two silica particles with different sizes. The consensus in the literature (for experiments, see, e.g., [1–5] and for theory [6,7] and references therein) is that, aside from those showing clear evidence of specific interactions (e.g., mixtures containing reverse micelles [8]), such suspensions behave essentially as binary HS mixtures. The behavior of the latter is governed by a small-spheres mediated effective interaction between the bigger spheres. Its most salient feature is a deep well at short separation that is associated with an increase of the free volume for the small particles, when the exclusion spheres of the big ones overlap. This is a special case of "depletion effects" that refer to situations in which the solvent is expelled from the inner space between sufficiently close macroparticles [9,10]. It will thus be referred to here as the HS depletion interaction. The special case of mixtures of colloids and ideal polymers and the related work based on the Asakura-Osawa model [9] (see Ref. [11] for a recent review) will not be discussed here. In mixtures of "hard-sphere-like" colloids, one expects a HS depletion effect associated with the small colloid effective hard-core diameter D_s. As D_s is much greater than the lengths associated with the other interactions felt by the big solutes, the HS depletion potential is supposed in the literature to be the main contribution to the effective interaction. Accordingly, the phase behavior of "hard-sphere-like" colloidal mixtures should be close—at least qualitatively—to that of pure HS mixtures. This conjecture is also based on the experimental observations that when the suspension involves only a single species of the same colloidal particles, it behaves nearly as a one-component HS system (with the same equation of state, critical values at melting, and crystallization) [3,11–13].

The purpose of this paper is precisely to question this "premise" in the specific case of the asymmetric mixture. First, it is generally difficult to anticipate in this case the complex interplay of non-HS contributions (see Refs. [14–17] for a discussion of true molecular solvent/colloid binary mixtures). Second, the fundamental features of the phase diagram of pure HS mixtures are critically dependent on the specific characteristics of the HS depletion well. In this work, we demonstrate that "small" non-HS interactions may have more consequences on the phase diagram than what is believed from the present consensus. The paper is thus organized as follows. In Sec. II, the method used to compute the phase diagram is specified. In Sec. III, we present our results for model interactions corresponding to specific situations that are discussed. These results are interpreted in Sec. IV. Section V is the conclusion.

II. METHODS

The model considered here is a highly asymmetric binary mixture of "small" and "big" particles (hereafter referred to by the indexes "*s*" and "*b*"). The corresponding physical systems will be specified in the next section. In all the situations considered in this paper, the fluid of small particles is assumed to remain in a single phase, irrespective of the big particles density ρ_b. The big particles phase behavior was thus determined in the effective one-component fluid (EOCF) representation. We briefly recall the main points of this well-known method. The convenient variables in this representation are those of the semigrand ensemble $(\mu_s; N_b, V, T)$, where μ_s is the chemical potential of the small particles, N_b is the number of big ones in the volume V, and T is the temperature. The free energy F of the mixture is

$$\beta F = -\ln\left(\mathrm{Tr}_{b,N_b}\left[\sum_{N_s}^{\infty} \mathrm{Tr}_{s,N_s}\{\exp[-\beta(H-\mu_s N_s)]\} \right] \right). \tag{1}$$

The total potential energy H is supposed to be pair additive: $H=H_{bb}+H_{sb}+H_{ss}$ with H_{ij} the total interaction potential be-

tween species i and j. $\beta=1/k_BT$ (with k_B Boltzmann's constant) and the symbol $\mathrm{Tr}_{\alpha,N_\alpha}$ designates the integral over the spatial coordiantes of the N_α particles of species α

$$\mathrm{Tr}_{\alpha,N_\alpha}[X]=\frac{1}{N_\alpha!\,\Lambda_\alpha^{3N\alpha}}\int\left(\prod_{i=1}^{N_\alpha}dr_i\right)X(r_{1,\cdots},r_{N\alpha}) \tag{2}$$

with $\Lambda_\alpha=h/\sqrt{2\pi m_\alpha k_BT}$. Equation (1) may be written as

$$\beta F=-\ln[\mathrm{Tr}_{b,N_b}\exp(-\beta H^{\mathrm{eff}})], \tag{3}$$

where

$$\exp(-\beta H^{\mathrm{eff}})=\sum_{N_s=1}^{\infty}\mathrm{Tr}_{s,N_s}\{\exp[-\beta(H-\mu_sN_s)]\}. \tag{4}$$

F may be interpreted as the free energy of an effective one-component fluid of big particles interacting through the effective Hamiltonian $H^{\mathrm{eff}}=H_{bb}+H^{\mathrm{ind}}$ with

$$\exp(-\beta H^{\mathrm{ind}})=\sum_{N_s=1}^{\infty}\mathrm{Tr}_{s,N_s}\{\exp[-\beta(H_{ss}+H_{sb}-\mu_sN_s)]\}. \tag{5}$$

H^{eff} is thus the sum of a direct interaction H_{bb} and an indirect one, H^{ind}, that is mediated by the fluid of small particles. The exact computation of the N_2-body interaction energy H^{ind} is not feasible. The usual approximation is then to expand Eq. (5) in terms of the grand potentials for the small particles without big ones $[\Omega_0(\mu_s,T,V)]$, in the presence of one big particle $[\Omega_1(\mu_s,T,V)]$, two big particles separated by a distance r $[\Omega_2(\mu_s,T,V,r)]$, etc. Up to the two-body terms, one gets (see, e.g., Ref. [6])

$$\exp(-\beta H^{\mathrm{ind}})=\Omega_0(\mu_s,T,V)+N_b\omega_1(\mu_s,T,V)+\exp\left(-\beta\sum_{i<j}\omega_2(r_{ij})\right), \tag{6}$$

where $\omega_1=\Omega_1(\mu_s,T,V)-\Omega_0(\mu_s,T,V)$ and

$$\omega_2(r_{ij})=\Omega_2(\mu_s,T,V,r_{ij})-\Omega_2(\mu_s,T,V,\infty) \tag{7}$$

is the potential of mean force (PMF) between two big particles at infinite dilution in the bath of small ones. Note that this pair interaction approximation seems sufficient for the HS or short-range potentials $u_{ij}(r)$ considered here (see, for example, [18] and references therein). As we are interested only in the phase behavior of the big particles, the useful part H' of H^{eff} is $H'=\Sigma_{i<j}[u_{bb}(r_{ij})+\omega_2(r_{ij})]$, where u_{bb} is the big particle direct interaction. This effective interaction is a function of μ_s, T, and V. Equivalently, it may be expressed as a function of $T$and the reduced density ρ_s^* of the small particles in the reservoir ($\rho_s^*=\rho_sD_s^3$). Thus, for a fixed temperature T, the theoretical phase diagram can be deduced from the free energy of the EOCF of big particles in the (ρ_s,ρ_b) plane.

To this end, one first computes the PMF at infinite dilution. The route based on the grand potential [Eq. (7)] is useful when a practical expression of the free energy is available, as in density-functional-theory calculations for hard spheres [19]. An alternative, which is more appropriate to models with attractive forces [20], is the expression of the PMF from the pair distribution function of the big particles at infinite dilution,

$$g_{bb}(r,\rho_b\to0)=\exp[-\beta u_{bb}(r)+\phi^{\mathrm{eff}}(r,\mu_1)]. \tag{8}$$

The formal proof of the equivalence of the two routes is given in Ref. [21], for example. To specify that we actually used this last route, the PMF is denoted by ϕ^{eff}. Details on the practical use of Eq. (8) are given in Ref. [20]. We mention here that one needs the pair distribution functions (PDF) $g_{ij}(r)$ for a mixture with $\rho_b\to0$. These were obtained from the Ornstein-Zernike equations (OZE) with the reference hypernetted-chain (RHNC) closure. The bridge functions we used were computed from Rosenfeld's density-functional theory [22] in the limit $\rho_b\to0$. The accuracy of this method has been positively checked against the simulation data of Refs. [17,23] for situations typical of solvent-colloid mixtures. We performed a similar test with interaction parameters corresponding to the pseudobinary mixtures considered in the literature as "HS-like." The results are satisfying (see the Appendix) for the purpose of this paper, which is to emphasize the qualitative changes with respect to the HS depletion scenario.

The free energy of an EOCF of particles interacting with ϕ^{eff} was computed in the (ρ_s,ρ_b) plane similarly as in Refs. [15,17]: for the fluid phase, the very accurate RHNC integral equations [24] were used with the bridge function of Malijevski and Labik [25] as unique input (see Ref. [26] for details). The free energy in the solid was computed in the variational perturbation theory. The accuracy of the hybrid method was shown in Ref. [15] for the fluid-solid (FS) and fluid-fluid (FF) transitions, by comparison with the simulation data of Dijkstra *et al.* [6], and confirmed more recently by simulations from our group [17] for the FF transition. Concerning a possible solid-solid (SS) transition between two solid states with different densities, it was shown in [26] that the perturbation treatment is suitable to describe a dense solid near close packing but is more problematic for a "softer" one with lower density. However, no SS transition involving such as soft solid will be observed in our results.

III. RESULTS

We begin by directly showing the main result of this study: in the specific case of pseudobinary mixtures, very small non-hard-core interactions can have an unexpected impact on the phase diagram. Three different situations are compared in Fig. 1 for a diameter ratio $q=10$: Fig. 1(a) is for a pure hard-spheres mixture. Figures 1(b) and 1(c), relative to systems with attractions, correspond, respectively, to the following models.

(1) A HS mixture with a very-short-range Yukawa tail in the small-big particle interaction:

$$\beta u_{sb}^{(1)}(r>D_{sb})=-\frac{\varepsilon^*}{r/D_s}\exp\{-\kappa_1(D_{sb}-r)\},$$

$$u_{sb}^{(1)}(r<D_{sb})=+\infty \tag{9}$$

with $D_{sb}=D_{sc}(q+1)/2$. The inverse interaction range $\kappa_1^*=\kappa_1D_s$ is specified in the table, and the contact value u_c^*

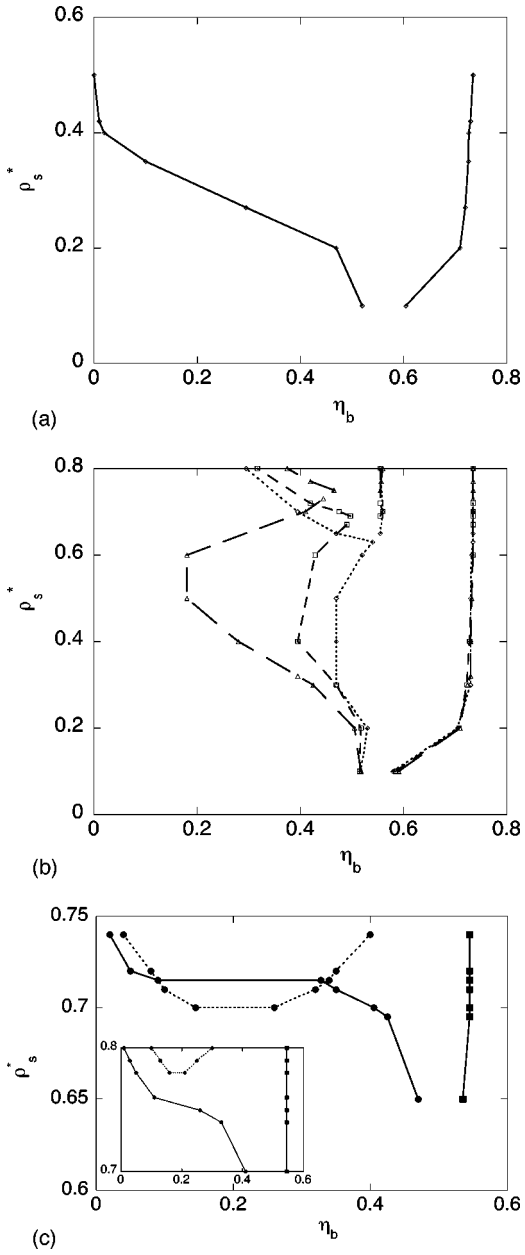

FIG. 1. Phase diagram of the big particle effective one-component fluid (EOCF) with $q=10$. (a) Hard spheres, fluid-solid transition. (b) Model (1): long dashes, $\kappa^*=100$; short dashes, $\kappa^*=60$, dots, $\kappa^*=40$. The nearly straight lines observed in the upper right region correspond to a solid-solid transition. (c) Model (2): line, fluid-solid transition; dots, fluid-fluid transition. The inset shows the same lines for a 9% smaller $\varepsilon_{\mathrm{LJ}}^*$. ρ_s^* is the small particle reduced density in the reservoir and η_b the big particle packing fraction.

$=-2\varepsilon^*/(q+1)$ is fixed to $u_c^*=-1.45$ in units of k_BT (*or* $\varepsilon^*=8$).

(2) HS macroparticles in a Lennard-Jones (LJ) fluid [17],

$$\beta u_{ss}(r>D_s)=4\varepsilon_{\mathrm{LJ}}^*\left[\left(\frac{D_s}{r}\right)^{12}-\left(\frac{D_s}{r}\right)^{6}\right]. \qquad (10)$$

The strength of the LJ potential was taken as $\varepsilon_{\mathrm{LJ}}^*=0.6$ and the other interaction potentials are a pure HS u_{bb} and a Yukawa u_{sb} with $u_c^*=-1.45$ and appropriate range (see Table I).

TABLE I. Parameters of the small-big Yukawa potential ($\kappa^*=\kappa D_s$). $\Delta B_{sb}^{(2)}=(B_{sb}^{(2)}-B_{sb,\mathrm{HS}}^{(2)})/B_{sb,\mathrm{HS}}^{(2)}$ is the change in the second virial coefficient from hard spheres ($B_{sb,\mathrm{HS}}^{(2)}$) to the Yukawa potential ($B_{sb}^{(2)}$).

Model	κ^*	$\Delta B_{sb}^{(2)}$
1	[40, 100]	[−3.1%, −1.3%]
2	2.5	−54.1%

Before analyzing the results show in Fig. 1, it is useful to stress first the essential difference between models (1) and (2): they correspond to widely different attraction ranges. This is obvious for u_{ss}. Now the range of u_{sb} is of the order of the "solvent" diameter in model (2): $\kappa_2^{-1}=0.4D_s$. For the same contact value u_c^*, it is much smaller in model (1): $0.01D_s\leqslant\kappa_1^{-1}\leqslant 0.025D_s$. A more visual illustration of this last situation is Fig. 2, which shows the attraction range at the appropriate scale [$\kappa_1^*=60$ in model (1)]. For what concerns the connection with real systems, models (1) and (2)—although very simple—may be related to two different classes of mixtures. Model (2) typically corresponds to a

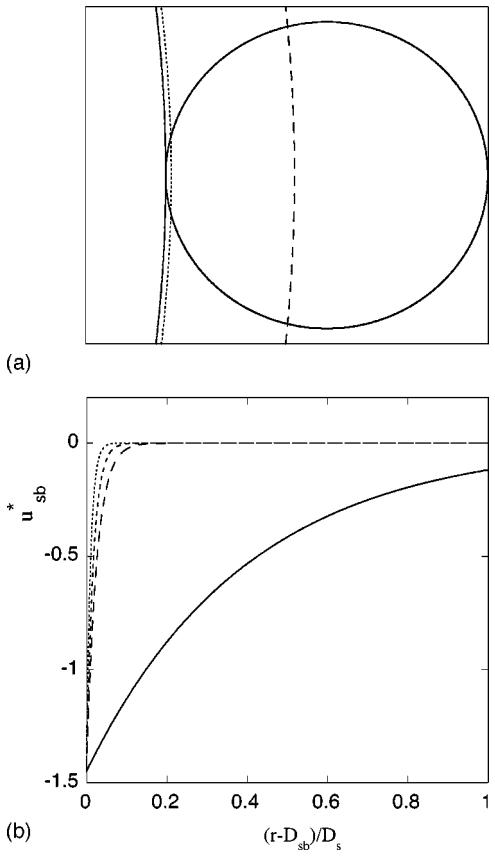

FIG. 2. Extension of the small-big attractive Yukawa tail for $\kappa=60/D_s$ and $\kappa=2.5/D_s$ at the scale of the small particle diameter D_s (a). The dots and dashes correspond to the separations for which $u_{sb}=u_c^*/e$ for $\kappa=60/D_s$ and $\kappa=2.5/D_s$, respectively. (b) u_{sb} versus $(r-D_{sb})/D_s$ for $k^*=100$, 60, 40, and 2.5.

"true" solute/solvent mixture: colloidal particles of one species suspended in a molecular solvent. The choice of an attractive interaction, u_{sb}, should be appropriate to sterically stabilized colloids: the attraction may correspond, for instance, to the van der Waals force between the solvent molecules and the microscopic objects forming the colloids and their surface layer. Since it is expected to operate at the scale D_s of the small (solvent) particles, it falls in the category described by model (2). This is the situation more often considered in the papers discussing the non-HS interactions effect in colloidal suspensions [14–17].

In contrast with this, the interaction range in model (1) corresponds to those colloidal mixtures that are classified in the literature as "hard-sphere-like." They involve two differently sized colloids (and a molecular solvent) having dimensions much greater than any other characteristic length in the suspension. As a result, the non-HS part of the intercolloidal interactions has a range much smaller than D_s, as in model (1). The values used here may be compared with the estimations found in the experimental literature: recently, the experimental phase diagram of mixtures of two differently sized silica particles grafted with stearyl alcohol and suspended in cyclohexane has been investigated [27]. One had $D_s=32$ nm and $D_b=185$ nm for the system classified as HS-like, having a stabilizing layer thickness of less than 2 nm (the exact value was not specified). Considering then an attraction range of, say, 1 nm due, for example, to the surface layers overlap, the values discussed here cover the range $40\ \text{nm} \leqslant D_s \leqslant 100\ \text{nm}$ for the small colloid diameter (and hence $0.4\ \mu\text{m} \leqslant D_b \leqslant 1\ \mu\text{m}$ for $q=10$). The ratio between the attraction range and the particle diameters in model (1) is thus probably even smaller than in the real system. Another example is the case of PMMA particles mixed with polystyrene studied in Ref. [28]. Here, the screening length characterizing the intercolloidal electrostatic repulsion was estimated to be $\kappa^{-1} \approx 3$ nm for $D_s=83$ nm (and $D_b=1.1\ \mu$m) or $\kappa^*=27$. The interaction range is again greater than in model (1). This shows that the interaction ranges selected for model (1) are truly representative of the "small" non-HS interactions observed in real systems.

The importance of the non-HS interactions in models (1) and (2) may also be assessed by comparing the associated second virial coefficient ($B_{sb}^{(2)}$) to the pure HS situation. For the Yukawa potential, which is monotonous, the deviation $\Delta B_{sb}^{(2)}=(B_{sb}^{(2)}-B_{sb,\text{HS}}^{(2)})/B_{sb,\text{HS}}^{(2)}$ from hard spheres ($B_{sb,\text{HS}}^{(2)}$) is indeed a global measure of the attraction strength. One finds $\Delta B_{sb}^{(2)}=-1.3-3.1\,\%$ with model (1) to be compared to $\Delta B_{sb}^{(2)} \approx -54\%$ for model (2). This last situation departs significantly from the pure HS case, whereas model (1) is very close to the HS limit. Note that the small values of $\Delta B_{sb}^{(2)}$ mean that the very short range considered here does not correspond to Baxter's "sticky" limit [29]. The interaction strength remains indeed here quite moderate. To emphasize again the actual smallness of $u_{sb}^{(1)}$, we have computed also $\Delta B^{(2)}$ for the—already very steep—direct interaction estimated in Ref. [12] by the surface force apparatus: we found $\Delta B^{(2)} \approx 3-18\,\%$ for spheres of diameter 800–100 nm.

As a final check of the adequacy of model (1) to a HS-like situation, we also considered the experimental results of [28]. In this study, the pair potential of PMMA particles mixed with charge-stabilized PS ones was directly measured (for another example, see Ref. [30]). At small PS density, the authors compared the theoretical HS depletion potential to the experimental values. They observed a deviation at contact, $\Delta\phi(D_b) \approx 30\%\,\phi^{\text{dep}}(D_b)$, although the screening length of the electrostatic repulsion δ was very small ($\delta \approx 3\% D_s$). We could reproduce this deviation by computing the PMF as in model (1) but with a repulsive tail having a range fixed to the experimental value: $1/\kappa_1^*=0.03$ and a contact value $u_c^*=+2.5$. This is certainly not excessive for a repulsive potential. It leads to a change of the associated second virial coefficient $\Delta B^{(2)} \approx 2.3\%$, which is comparable to those found for model (1).

Finally, we mention also the study in Ref. [31] of the modification of the effective potential induced by nonadditivity of the hard-core diameters. The values of $\Delta B_{sb}^{(2)}$ in the table are similar to those obtained with the smaller nonadditivity, corresponding roughly to $\delta \approx 3-10\,\% D_{sc}$. In Ref. [32], the influence of Yukawa heteroattractions with ranges $1/\kappa^*=0.05$ and 0.1 was also computed at the level of the effective potential.

This discussion shows that although model (1) is an idealized one, the values of the parameters that we have selected are indeed representative of "hard-sphere-like" situations, as observed in real systems. These "residual" interactions are usually considered as irrelevant in the literature. Therefore the features of the phase diagram associated with this situation and illustrated in Fig. 1(b) should constitute a good test of the validity of the HS mixture as a sensible physical limit. The main information provided by Fig. 1 appears now more clearly.

(1) The phase diagram shown in Fig. 1(a), obtained from the methods described in Sec. II, shows the same features as those described in the literature [6,15,33]. We summarize here the main points: the absence of a stable FF transition and the broad FS coexistence domain that appears at rather low small particles density: for $\rho_s^* \geqslant 0.4$, the EOCF separates into a dilute gas in equilibrium with a solid near close packing.

(2) Before discussing Fig. 1(b) in more detail, we briefly describe the phase diagram of model (2) [Fig. 1(c)] that was obtained in Ref. [17]. One observes first a considerable extension of the stability domain of the fluid phase. Second, for a suitable choice of the parameters, a significant domain corresponds to a stable FF coexistence. It is now well established that in this regime, non-HS interactions may lead to a rich variety of phase behavior landscapes by changing the magnitude or range of the potentials $u_{\alpha\beta}(r)$ [see the inset, the effect of a small change in $\varepsilon_{\text{LJ}}^*$].

(3) The phase diagram shown in Fig. 1(b) is, to our knowledge, the first one computed for nearly HS interactions. This has not been done before precisely because the residual interaction beyond the hard core is usually considered as negligible. The deviations from the pure HS phase diagram in Fig. 1(b) are quite unexpected given the very "small" addition to the HS potential in model (1) (recall here the very low change of the second virial coefficient). The interesting features observed in the upper part of the diagram

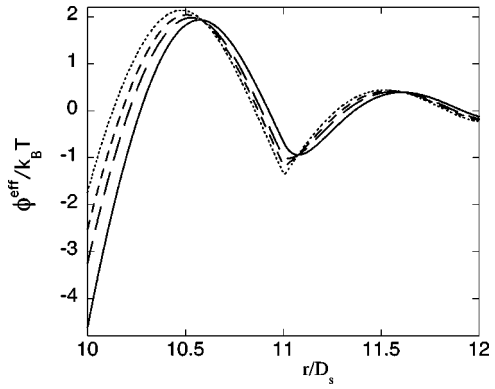

FIG. 3. Potential of mean force $\phi^{\text{eff}}/\kappa_B T$ for model (1) with small colloid density $\rho_s^*=0.6$. From top to bottom at contact: $\kappa^*=40$, 60, and 100 (line =HS).

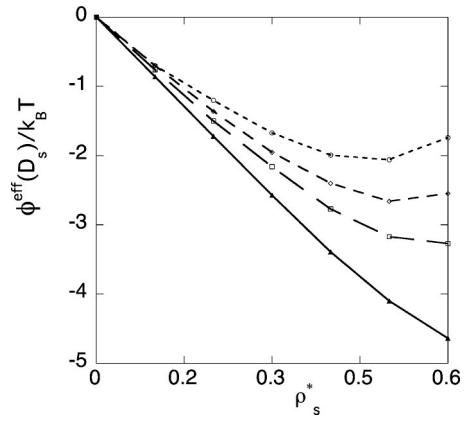

FIG. 4. Influence of the small colloid–big colloid Yukawa tail on the contact value of the effective potential in model (1). From top to bottom: $\kappa^*=40$, 60, and 100 (line =HS).

will not be discussed here. Some caution is indeed required here since the accuracy of the RHNC ϕ^{eff} has not been tested in this region of relatively high ρ_s^* [see Fig. 6(a) in the Appendix]. For $\rho_s^* \leqslant 0.65$, one observes first that the metastable FF transition found for $\rho_s^* \geqslant 0.55$ with the HS mixture [6,15] is removed by the attractive tail. Furthermore, a significant extension of the fluid phase is again observed, although it is less important than for model (2) in the range $0 \leqslant \rho_s^* \leqslant 0.6$. While the broadening of the FS coexistence domain starts for a value of ρ_s^* that is rather close to that of hard spheres, the crystallization line strongly departs from that model when ρ_s^* increases (below $\kappa^*=40$, no broadening is observed). Above $\rho_s^* \approx 0.5$, the slope of the crystallization line reverses, leading to a reentrant fluid phase. In this region, the fluid phase may be stable even up to greater values of η_b than for model (2). For the melting line, no significant change is observed for $\rho_s^* \leqslant 0.65$.

Then, while one would have expected the phase behavior of model (1) to closely resemble that of hard spheres, qualitative differences are actually observed as with model (2). Recall that the latter corresponds to much greater contributions of the attractions (expressed, for instance, by the second virial coefficient).

IV. INTERPRETATION

To analyze these results, it is first useful to recall the HS scenario: in that case, the main features of the phase diagram in the (ρ_s^*, η_{bc}) plane are closely related to the depth and the range of the well shown near contact by the depletion potential ϕ^{dep}.

Indeed, the rapid increase of $\phi^{\text{dep}}(D_b)$ (Figs. 3 and 4) with ρ_s^* and the simultaneous sharpening of the well leads for $\rho_s^* \geqslant 0.2$ (when $q=10$) to a separation of the big colloids fluid into a dilute vapor governed by entropy and a close-packed solid governed by energy [6,15] as in simple fluids with short-range attraction. The close-packed solid is of course favored by the large value of $\phi^{\text{dep}}(D_b)$. In this state indeed, the energy per particle is roughly $E \approx 1/2 z \phi^{\text{dep}}(D_b)$, $z=12$ being the number of nearest neighbors. The rapid increase of $\phi^{\text{dep}}(D_b)$ with ρ_s^* is then reflected by the onset of a sharp minimum in the solid branch of the free-energy curve F^s [see Fig. 5(a)]. As ρ_s^* increases, its depth becomes very important with respect to the variations of the free energy occurring at lower density. Indeed, states with intermediate density do not take advantage of the attractive well, which is too narrow. The common tangent construction is thus possible only be-

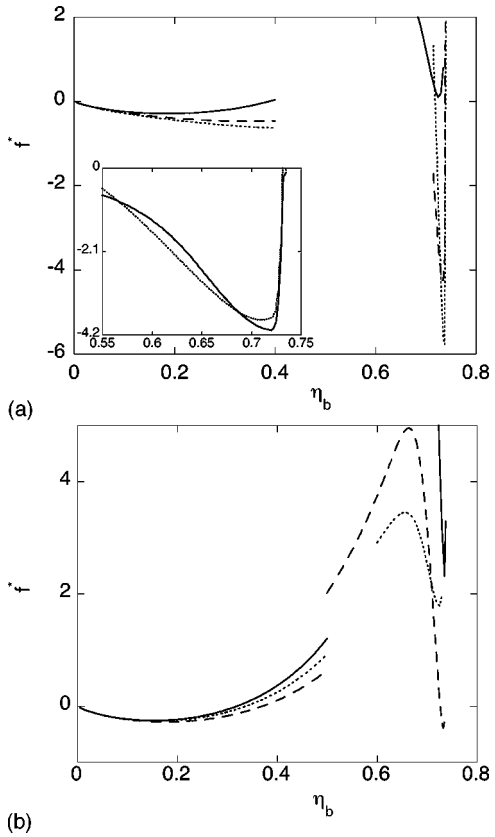

FIG. 5. Reduced free energy $f^*=D_b^3 F/\kappa_b T\, V$ for HS (a) and for model (1) with $\kappa^*=100$ (b). F is the EOCF free energy. Line, $\rho_s^*=0.32$; dashes, $\rho_s^*=0.5$; dots, (a) $\rho_s^*=0.7$. Inset in (a): Influence of the long-range part of the HS depletion potential on the free energy of the HS solid. Line, full RHNC depletion potential. Dots, same potential truncated at $r=D_b+D_s$.

tween densities corresponding to a very dilute gas and a close-packed solid. The FS coexistence domain widens then very quickly with ρ_s^*. The effect of the residual tails is precisely to break this scenario that is essentially due to the "singularity" of the HS depletion well. The minimum of the solid free energy is now shifted [Fig. 5(b)] roughly by $\Delta F = 6N_b \Delta\phi(D_b)$, where $\Delta\phi = \phi^{\text{eff}} - \phi^{\text{dep}}$ (this perturbative view is valid near close packing [26]). As $\Delta\phi > 0$, one has $\Delta F > 0$. For the "small" interactions considered here, however, one might have expected this contribution to be dominated by ϕ^{dep}, leading thus to moderate shifts of the transition lines. On the contrary, when comparing ϕ^{eff} to ϕ^{dep} (see Figs. 3 and 4), the weight of $\Delta\phi$ is found to increase strongly with ρ_s^*. Above $\rho_s^* \approx 0.5$, this eventually leads to an inversion in the variation $\phi^{\text{eff}}(D_b)$, which is the direct origin of the reentrance observed in the phase diagram. In addition, the removal of the FF metastable transition line is also a consequence of the strong reduction of the depletion well, the energy gain corresponding to a liquid density being then insufficient.

We emphasize here that it is actually the sharpness of the depletion well that determines the main features of the HS mixture phase diagram. On the contrary, this phase diagram does not seem to be significantly affected by the longer-range oscillatory part, $\phi^{\text{dep}}(r \geq D_b + D_s)$: indeed, the phase diagram of Fig. 1(a) computed from the full RHNC depletion potential is very close to that obtained in Ref. [15] with the potential of Götzelmann *et al.* [34], which is truncated at $r = D_b + D_s$ (the EOCF free energy was computed in the same way). This striking difference between the respective effects of the depletion well and the longer-range oscillatory part may be understood by recalling that, in the close packing solid described above, the internal energy is determined essentially by $\phi^{\text{dep}}(D_b)$ $[E \approx 1/2z\phi^{\text{dep}}(D_b)]$ and not by $\phi^{\text{dep}}(r \geq D_b + D_s)$. This is illustrated in the inset of Fig. 5(a) that shows, for $\rho_s^* = 0.5$, the very small effect on the minimum F_s of truncating the HS depletion potential beyond $D_b + D_s$. Of course, the dilute gas is itself weakly affected by truncation of the interaction potential. Hence, the hard-sphere mixture phase diagram is very sensitive to those "details" of the depletion potential that concern the well at contact but not to its long-range part.

Figure 1(b) illustrates then the modifications—at the qualitative level—of the phase behavior that may arise from residual non-HS heteroattractions. We have checked that adding a tail to the interaction between the small colloids induces also effects that increase with ρ_s^*. Thus, although the phase diagram shown in Fig. 1(b) is specific to model (1), strong deviations from the HS scenario can be expected in general in systems usually classified as HS-like. In this respect, experimental phase diagrams of model mixtures of sterically stabilized silica particles have been recently reported [27]. For the system having typical characteristics of an "HS-like" situation (see above), significant deviations from the HS fluid phase boundary were found for the higher values of the small particles density. Our present results suggest similar trends that we plan to examine in more detail in the future. Finally, we note that our conclusions do not corroborate the conjectures made in Ref. [19]. The authors analyzed there the effect of small nonadditivity on the effective potential and the associated second virial coefficient. They argued that the deviations from the additive HS mixture should hardly be observable at the level of the phase diagram, due to the uncertainty in the definition of the colloids packing fraction. This reasoning assumes that the modifications due to residual interactions should be purely quantitative. On the contrary, our present results suggest qualitative changes in the phase behavior with respect to additive hard spheres.

V. CONCLUSION

The results presented in this paper show that the commonly admitted view according to which mixtures of the so-called "hard-sphere-like" colloids may safely be modeled as hard sphere mixtures is disputable. A first analysis based on the sizes of the particles would indeed have considered *residual* non-hard-sphere interactions existing in these suspensions as irrelevant "decorations" of the hard spheres. On

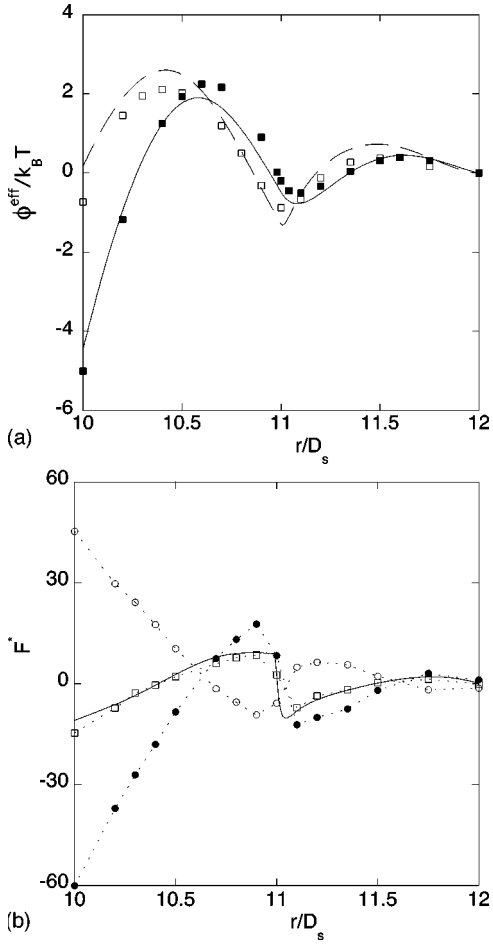

FIG. 6. (a) Potential of mean force for a mixture with $q = 10$ and $\rho_s^* = 0.585$. RHNC, curves; simulation, symbols; HS, line and full squares (see also [35]); Yukawa tail with $\kappa^* = 20$, dashes and open squares. (b) Mean force for the Yukawa tail with $\kappa^* = 20$. Symbols, simulation; full circles, F_{HS}^*; empty circles, F_{attr}^*; squares, total force $F^* = F_{\text{HS}}^* + F_{\text{attr}}^*$. The dashed lines connecting the simulation points are guides to the eyes. Line, RHNC total force.

the contrary, the situations considered here provide clear evidence that such interactions may lead to qualitative changes with respect to hard spheres in the phase diagram. Previous studies have underlined the natural insufficiency of the HS scenario in the context of pure solvent–sterically stabilized solute systems. This was explained by the fact that the various non-HS interactions (e.g., dispersion forces) have ranges comparable with the solvent diameter. This work raises now the issue of the extreme sensitivity of the HS depletion scheme with respect to small departures from the pure hard-sphere interaction. This scenario is indeed so tightly linked to the singularity of the hard-core potential that "decorated" hard colloids behave quite differently from ideally hard ones. Although this sensitivity to "details" in the interactions raises the question of the feasibility of quantitative calculations for real systems, its observation should also stimulate further studies with the aim of determining more precisely the parameters that are actually relevant in these systems. This issue is of practical relevance, since the effective interactions in colloidal systems can be controlled to some extent. In mixtures containing two colloidal species with different radii, it is conceivable that the non-hard-sphere interactions—for example between unlike species as discussed above—might also be tuned by acting on the chemical composition or the structure of the colloids surface layers (e.g., [27]). Progress in this direction might provide practical ways to control the thermodynamics of these complex systems.

APPENDIX: RHNC POTENTIAL OF MEAN FORCE VERSUS SIMULATION

In order to check the accuracy, for the short-range interactions of this study, of the PMF computed by the method introduced in Ref. [20] and outlined in Sec. II, we performed Monte Carlo simulations. As detailed in Ref. [17], we obtained ϕ^{eff} following the method of Dickman *et al.* [36], whose direct output is the mean force between two fixed big particles:

$$F(r) = \left\langle \sum_{1}^{N_1} \cos\,\theta \right\rangle_{\mathrm{contact}} + \left\langle \sum_{1}^{N_1} \frac{\partial u_{sb}(u)}{\partial u} \cos\,\theta \right\rangle.$$

Figure 6(a) shows ϕ^{eff} obtained by numerically integrating the mean force for $\kappa^{*}=20$ (the simulations become increasingly difficult as the range of the interaction decreases). The uncertainty in $\phi^{\mathrm{eff}}(r)$ obtained by integrating the MC force sums the uncertainty on the force over all the integration points [shown by symbols in Fig. 6(b)] beyond r. The main source of uncertainty in the force lies now in the extrapolation to $r=D_{sb}$of the HS contribution (first term in brackets). There is no problem with the second term. In the example shown below, the reduced force at contact $F^{*}=FD_s/\kappa_B T=-15$ results from a HS contribution estimated to $F^{*}_{\mathrm{HS}}\approx -60$ and the tail contribution $F^{*}_{\mathrm{attr}}\approx 45$. The final uncertainty on ϕ^{eff} from simulation is thus difficult to asses, as are the discrepancies that are visible near contact in Fig. 6(a) between RHNC and simulation. Nevertheless, the deviation $\Delta\phi=\phi^{\mathrm{eff}}-\phi^{\mathrm{dep}}$ is well reproduced (4.6 $\kappa_B T$ and $\approx 4.3\ \kappa_B T$, respectively).

[1] J. S. van Duijneveldt, A. W. Heinen, and H. N. W. Lekkerkerker, Europhys. Lett. **21**, 369 (1993).
[2] P. D. Kaplan, J. L. Rouke, A. G. Yodh, and D. J. Pine, Phys. Rev. Lett. **72**, 582 (1994).
[3] A. D. Dinsmore, A. G. Yodh, and D. J. Pine, Phys. Rev. E **52**, 4045 (1995).
[4] E. H. A. de Hoog, W. K. Kegel, A. van Blaaderen, and H. N. W. Lekkerkerker, Phys. Rev. E **64**, 021407 (2001).
[5] T. Eckert and E. Bartsch, Phys. Rev. Lett. **89**, 125701 (2002).
[6] M. Dijkstra, R. van Roij, and R. Evans, Phys. Rev. E **59**, 5744 (1999); M. Dijkstra, Curr. Opin. Colloid Interface Sci. **6**, 372 (2001).
[7] R. Roth, R. Evans, and S. Dietrich, Phys. Rev. E **62**, 5360 (2000).
[8] J. L. Parker, P. Richetti, P. Kékicheff, and S. Sarman, Phys. Rev. Lett. **68**, 1955 (1992).
[9] S. Asakura and F. Oosawa, J. Chem. Phys. **22**, 1255 (1954).
[10] A. Vrij, Pure Appl. Chem. **48**, 471 (1976).
[11] W. C. K. Poon, J. Phys.: Condens. Matter **14**, R859 (2002).
[12] G. Bryant, S. R. Williams, L. Quian, I . K. Snook, E. Perez, and F. Pincet, Phys. Rev. E **66**, 060501(R) (2002).
[13] A. Yethiraj and A. van Blaaderen, Nature (London) **421**, 513 (2003).
[14] S. Amokrane, J. Chem. Phys. **108**, 7459 (1998).
[15] J. Clément-Cottuz, S. Amokrane, and C. Regnaut, Phys. Rev. E **61**, 1692 (2000).
[16] A. A. Louis, E. Allahyarov, H. Löwen, and R. Roth, Phys. Rev. E **65**, 061407 (2002).
[17] J. G. Malherbe, C. Regnaut, and S. Amokrane, Phys. Rev. E **66**, 061404 (2002).
[18] S. Amokrane, A. Ayadim, and J. G. Malherbe, J. Phys.: Condens. Matter **15**, S3443 (2003).
[19] R. Roth, R. Evans, and S. Dietrich, Phys. Rev. E **62**, 5360 (2000).
[20] S. Amokrane and J. G. Malherbe, J. Phys.: Condens. Matter **13**, 7199 (2001); **14**, 3845(E) (2002).
[21] A. J. Archer and R. Evans, J. Chem. Phys. **118**, 9726 (2003).
[22] Y. Rosenfeld, J. Chem. Phys. **98**, 8126 (1993).
[23] H. Shinto, M. Miyahara, and K. Higashitani, J. Colloid Interface Sci. **209**, 79 (1999).
[24] F. Lado, S. M. Foiles, and N. W. Ashcroft, Phys. Rev. A **28**, 2374 (1983).
[25] A. Malijevsky, and S. Labik, Mol. Phys. **60**, 663 (1987); S. Labik and A. Malijevski, *ibid.* **67**, 431 (1989).
[26] P. Germain and S. Amokrane, Phys. Rev. E **65**, 031109 (2002).
[27] Y. Hennequin, M. Pollard, and J. S. van Duijneveldt, J. Chem.

Phys. **120**, 1097 (2004).
[28] J. C. Crocker, J. A. Matteo, A. D. Dinsmore, and A. G. Yodh, Phys. Rev. Lett. **82**, 4352 (1999).
[29] R. J. Baxter, J. Chem. Phys. **48**, 2770 (1968).
[30] R. Verma, J. C. Crocker, T. C. Lubensky, and A. G. Yodh, Phys. Rev. Lett. **81**, 4004 (1998).
[31] R. Roth, R. Evans, and A. A. Louis, Phys. Rev. E **64**, 051202 (2001).
[32] P. Germain, C. Regnaut, and S. Amokrane, Phys. Rev. E **67**, 061101 (2003).
[33] N. G. Almarza and E. Enciso, Phys. Rev. E **59**, 4426 (1999).
[34] B. Götzelmann, R. Evans, and S. Dietrich, Phys. Rev. E **57**, 6785 (1998).
[35] T. Biben, P. Bladon, and D. Frenkel, J. Phys.: Condens. Matter **8**, 10 799 (1996).
[36] R. Dickman, P. Attard, and V. Simonian, J. Chem. Phys. **107**, 205 (1997).